Neuroscience 262 (2014) 40–52

FUNCTIONAL REGENERATION OF INTRASPINAL CONNECTIONS IN A NEW *IN VITRO* MODEL ☆

M. HEIDEMANN, J. STREIT AND A. TSCHERTER*

Department of Physiology, University of Bern, Bühlplatz 5, 3012 Bern, Switzerland

Abstract—Regeneration in the adult mammalian spinal cord is limited due to intrinsic properties of mature neurons and a hostile environment, mainly provided by central nervous system myelin and reactive astrocytes. Recent results indicate that propriospinal connections are a promising target for intervention to improve functional recovery. To study this functional regeneration *in vitro* we developed a model consisting of two organotypic spinal cord slices placed adjacently on multi-electrode arrays. The electrodes allow us to record the spontaneously occurring neuronal activity, which is often organized in network bursts. Within a few days *in vitro* (DIV), these bursts become synchronized between the two slices due to the formation of axonal connections. We cut them with a scalpel at different time points *in vitro* and record the neuronal activity 3 weeks later. The functional recovery ability was assessed by calculating the percentage of synchronized bursts between the two slices. We found that cultures lesioned at a young age (7–9 DIV) retained the high regeneration ability of embryonic tissue. However, cultures lesioned at older ages (>19 DIV) displayed a distinct reduction of synchronized activity. This reduction was not accompanied by an inability for axons to cross the lesion site. We show that functional regeneration in these old cultures can be improved by increasing the intracellular cAMP level with Rolipram or by placing a young slice next to an old one directly after the lesion. We conclude that co-cultures of two spinal cord slices are an appropriate model to study functional regeneration of intraspinal connections.

Key words: spinal cord, organotypic cultures, multi-electrode array, regeneration.

INTRODUCTION

The adult spinal cord of higher vertebrates fails to regenerate after injury. This has been attributed to an inhibitory environment provided, for example, by myelin associated proteins such as Nogo-A, oligodendrocyte myelin glycoprotein and myelin associated glycoprotein (McKerracher et al., 1994; Mukhopadhyay et al., 1994; Chen et al., 2000; GrandPré et al., 2000; Prinjha et al., 2000; Kottis et al., 2002; Wang et al., 2002) or proteins associated with the extracellular matrix like chondroitin sulfate proteoglycans (CSPGs) (Levine, 1994). In addition, it has been shown that the age of a neuron can play an essential role in limiting axon regeneration. For example, Blackmore and Letourneau (2006) demonstrated with E9 and E15 brainstem explants of chicks that the axons growing from the older explants paused more often and advance more slowly than axons originating from the younger explants when grown on identical substrates. Therefore, the inhibitory environment and the state of neuronal maturation both seem to account for the failure of regeneration in the spinal cord. With their co-culture model Blackmore and coworkers found a 55% reduction in axon regeneration due to spinal cord environment inhibition while maturation of hindbrain neurons caused a 90% reduction. To which extent which factor contributes in other animals and other fiber tracts is not clear.

For many studies, descending tracts, especially the corticospinal tract have been the model systems of choice to investigate regeneration after spinal cord injury (SCI). However, recent results point to a pivotal role of propriospinal connections in the spontaneous recovery of function after incomplete spinal cord lesions (Bareyre et al., 2004; Courtine et al., 2008). Bareyre et al. (2004) demonstrated that after an incomplete SCI, severed corticospinal tract axons form connections with propriospinal neurons that are spared by the lesion and therefore still have intact axons. Thereby, a detour circuit around the lesion site can be formed allowing the transmission of descending signals below the damaged region. Furthermore, propriospinal neurons seem to respond better than descending tracts to certain treatments such as application of growth factors or tissue grafting (Houle, 1991; Xu et al., 1995; Blesch et al., 2004). Because of these characteristics, propriospinal fibers are a suitable target for therapeutic interventions to promote functional recovery after SCI. However, it is difficult to study the contribution of these fibers to regeneration in isolation without the

*Corresponding author. Address: Institut für Physiologie, Universität Bern, Bühlplatz 5, 3012 Bern, Switzerland. Tel: +41-631-87-12.
E-mail addresses: heidemann@pyl.unibe.ch (M. Heidemann), streit@pyl.unibe.ch (J. Streit), tscherter@pyl.unibe.ch (A. Tscherter).

Abbreviations: chABC, chondroitinaseABC; CSPG, chondroitin sulfate proteoglycans; CV, coefficient of variation; DAPI, 6-diamino-2-phenylindole; Dis, disinhibition; DIV, days *in vitro*; DRG, dorsal root ganglion; Hepes, 2-[4-(2-hydroxyethyl)piperazin-1-yl]ethanesulfonic acid; MEA, multi-electrode array; NgR-1, Nogo receptor 1; PBS, phosphate-buffered saline; SCI, spinal cord injury; StdC, standard conditions; TTX, tetrodotoxin.

0306-4522/13 $36.00
http://dx.doi.org/10.1016/j.neuroscience.2013.12.051

interference of ascending and descending fiber tracts. Bonnici and Kapfhammer (2008) used longitudinal spinal cord slices consisting of several segments to study their structural recovery. After setting lesions they stained the cultures with an anti-neurofilament SMI-31 antibody and estimated the amount of fibers crossing through the lesion center. However, the functional implications of this axonal regrowth are not known. So far, no *in vitro* model exists that allows the investigation of functional regeneration of propriospinal fibers. Here, we present a newly developed model based on two transversal spinal cord slices from 14-day-old rat embryos (E14) co-cultured adjacently on multi-electrode arrays (MEAs). Within a few days, the two slices connect to each other with axonal fibers that can subsequently be cut for further investigation.

We have previously shown that spontaneous bursting activity appears in organotypic spinal cord cultures, originating from intrinsic spiking and recurrent excitation and reflecting the activation of a neuronal network in the slice (Tscherter et al., 2001; Darbon et al., 2002; Czarnecki et al., 2008). In this study, we use the percentage of synchronized bursts between both slices 2–3 weeks after lesions to quantify functional regeneration. Moreover, the model offers the advantage of circumventing the need for large animal cohorts often required to test the efficacy of strategies to promote regeneration after SCI *in vivo*.

EXPERIMENTAL PROCEDURES

Culture preparation

Organotypic cultures were obtained from spinal cords of 14-day-old rat embryos (E14) from either Wistar rats purchased from Janvier (Le Genest St Isle, France) or Lewis rats expressing GFP ubiquitously in most organs (Inoue et al., 2005), kindly obtained from Professor St. Leib (University of Bern). The embryos were delivered by cesarean section from deeply anaesthetized animals (0.4 ml pentobarbital i.m., Streuli Pharma SA, Switzerland) and sacrificed by decapitation. The mother animals were sacrificed by intracardiac injection of pentobarbital. This procedure guaranteed a minimal suffering of animals (grade 0). The number of animals used to prepare the cultures was kept minimal. Animal care was in accordance with guidelines approved by Swiss local authorities (Amt für Landwirtschaft und Natur des Kantons Bern, Veterinärdienst, Sekretariat Tierversuche, approval Nr. 52/11). These guidelines are in agreement with the European Community Directive 86/609/EEC. The backs of the embryos were isolated from their limbs and viscera and cut into 225-μm-thick transverse slices with a tissue chopper. After dissecting the spinal cord slices from the surrounding tissue two of them were fixed next to each other on top of each MEA (Qwane Biosystems, Lausanne, Switzerland) by using reconstituted chicken plasma coagulated by thrombin (both Sigma–Aldrich, Switzerland). The slices were arranged with the ventral parts facing each other on each side of the 300-μm-wide groove located in the middle of the MEAs. The cultures were maintained in sterile plastic tubes containing 3 ml of nutrient medium and incubated in roller drums rotating at 2 rpm in a 5% CO_2-containing atmosphere at 36.5 °C (Streit et al., 1991). The medium was composed of 79% Dulbecco's modified Eagle's medium with Glutamax, 10% horse serum (both Gibco BRL, Switzerland), 10% H_2O and 5 ng/ml 2.5S nerve growth factor (Sigma–Aldrich, Switzerland). Half of the medium was replaced once to twice per week.

Experimental design and recordings

During the next few days *in vitro* (DIV) the slices grew and fused with each other. In most cultures, we performed a complete lesion with a scalpel to separate the two slices at the location of the groove within 8–28 DIV (Fig. 1A, B). This cut split the cultures in such a way that the slices were not touching each other anymore and their distance maximally reached the size of the groove width. The cultures were incubated further for at least 2 weeks until the activity was measured.

For the recordings the MEAs were mounted on an inverted microscope and kept in a bath of extracellular solution containing (in mM) NaCl 145; KCl 4; $MgCl_2$ 1; $CaCl_2$ 2; HEPES 5; Na-pyruvate 2; glucose 5 (pH 7.4). Recordings with extracellular solution are called ''standard condition''. Under ''disinhibition'' gabazine (10 μM) and strychnine (1 μM, both Sigma–Aldrich, Switzerland) were added to the extracellular solution. The bath was exchanged after every recording session, which lasted 10 min and was made at room temperature.

The MEAs are composed of a glass substrate, indium-tin oxide electrodes and an SU-8 polymer insulation layer. The recording site consists of 68 electrodes arranged in a rectangular grid. The electrodes were 40 × 40 μm in size and were spaced 200 μm apart (center to center, Fig. 1B). The electrode grid is split into two zones by the groove that is free of electrodes, electrical leads and insulation. The amplified signals from the 68 platinum electrodes are visualized and stored using custom-made virtual instruments within Labview (National Instruments, Switzerland). The analysis is performed offline with the software package IGOR (WaveMetrics, Lake Oswego, OR, USA).

Electrical stimulation was performed under disinhibition with the MEA electrodes with monopolar biphasic stimuli (duration = 1 ms, amplitude = 1.5–2.8 V), delivered from a custom-made stimulator.

Analysis of bursting activity

The extracellularly detected signals are fast voltage transients (< 4 ms) corresponding to action potentials in neuronal somata or axons. They are represented by single time markers called events. Raster plots show the events for each individual electrode (Fig. 1C). They can be transformed into network activity plots, which display the total activity recorded by all selected electrodes, summed within a sliding window of 10 ms, shifted by 1-ms steps (Fig. 1D) (Tscherter et al., 2001). Usually, fast voltage transients appeared in clusters and on several electrodes. We call these clusters bursts.

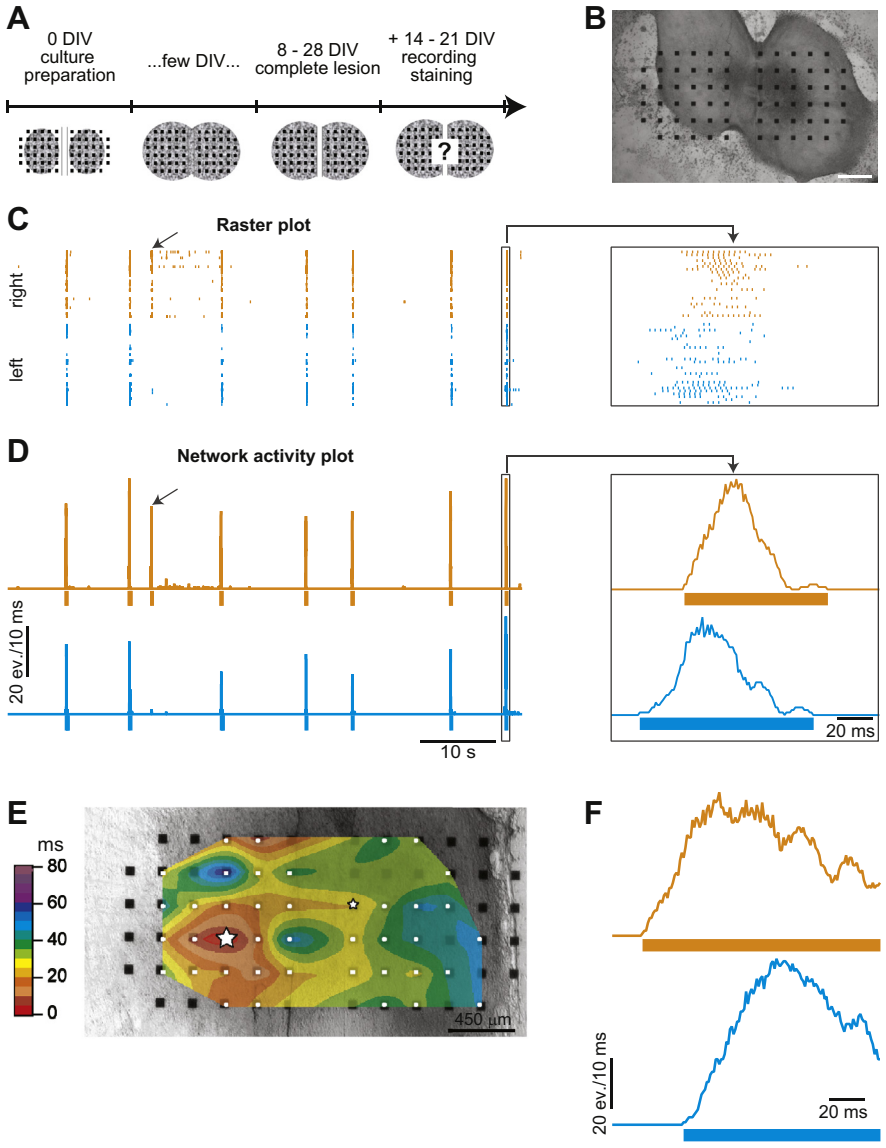

Fig. 1. Synchronized bursting activity at 8 DIV. (A) Timeline of experiments: We place two spinal cord slices next to each other on a MEA at 0 DIV. Within a few days, growing axons connect the two slices with each other. We cut these fibers with a scalpel in a time frame of 8–28 DIV. About 14 days later, we record the activity of the slices and afterward, fix the slices for immunohistochemical staining. (B) Bright-field image of two slices cultured for 6 days. They grew and fused along the sides facing each other. No lesion has been performed so far. The slice on the left shifted a little upward which left some electrodes at the bottom and the left side uncovered. Such electrodes are deactivated before the beginning of a recording session. Scale bar = 400 µm. (C) In the raster plot the recorded activity (standard conditions) is displayed separately for each individual electrode. The recordings come from an 8-DIV-old culture without lesion. The arrow refers to a burst not propagating from the right slice into the left. The magnification on the right shows the last burst pair. The single time markers (“events”) can be distinguished. (D) Raster plots can be transformed into network activity plots which display the total activity recorded by all selected electrodes. The bars below the baseline mark the beginning and the end of each burst for the left and the right slice. The magnification on the right shows again the last burst pair. ev. = events. (E) Spatiotemporal characterization of the burst propagation. The different shadings indicate the time needed by the wavefronts to reach the different electrodes. The stars indicate the burst starts in both slices. (F) Network activity plot of the initial phase of a synchronized burst pair recorded under disinhibition. The peak activity is higher under disinhibition than under standard conditions (compare to magnification in D).

To quantify the degree of functional connection between the two slices in the cultures, we calculated the percentage of synchronized bursts between them. First of all, bursts were detected for each side separately. A burst start was defined by being the first event in a time window of at least 5 ms, a burst end by being the last event in a time window of at least 25 ms. We only took bursts into account reaching the threshold of one quarter of the maximal burst size averaged from all bursts from the according side. To check if bursts were propagating over the midline we calculated the latencies between a burst start in one slice and the following burst start in the other. An accurate calculation of the latencies was ensured by a spatiotemporal characterization of burst propagation within the cultures, described in detail by Tscherter et al. (2001). A burst pair was termed “synchronized” when the latency was smaller than the average burst length. Especially in

co-cultures with a lot of activity, it is possible that both sides coincidentally initiate a burst in the chosen latency window. The number of randomly expected synchronized bursts (B_{RAN}) within the chosen latency window (w) during the whole recording (t) was calculated by $B_{RAN} = B_r * B_l * w/t$ for each side where B = number of bursts, r = right, l = left. We also determined for both sides separately the maximal number of bursts that can propagate to the second slice (B_{MAX}) by taking the number of burst starts of one side and subtracting the number of bursts initiated by the other side. The percentage of propagating bursts of each side (P_s) was then determined by $P_s = 100(B_{PROP} - B_{RAN})/(B_{MAX} - B_{RAN})$ where B_{PROP} = number of detected propagating bursts. The resulting two percentage numbers were used for the mixed cultures to distinguish what percentage of the synchronized bursts originated from the young and old slice, respectively. The total percentage of synchronized bursts per culture (P_T) was determined by $P_T = 100 (B_{PROPr} + B_{PROPl} - 2 * B_{RAN})/(B_{MAXr} + B_{MAXl} - 2 * B_{RAN})$.

To characterize the patterns of spontaneous bursting activity, the burst parameters from the following culture groups were analyzed (see 'Results' and Table 1): cultures without lesion recorded at 8–9 DIV, 21–23 DIV and 34–41 DIV, cultures with lesion applied at 7–9 DIV and recorded at 22–27 DIV and cultures with lesion applied at 21–23 DIV and recorded at 36–42 DIV. For simplicity, culture groups are cited as ''8 DIV'', ''22 DIV'' and ''36 DIV'' for cultures without any lesion and as ''22 DIV with lesion at 8 DIV'' and as ''36 DIV with lesion at 21 DIV''. To define the burst parameters for a single culture, we averaged the values from both slices within the culture.

Pharmacological treatment of spinal cord cultures after lesion

Inosine (1–10 μM, Sigma–Aldrich, Switzerland), NEP1–40 (9 μM, Sigma-RBI, USA), Nogo-A antibody (10 μg/ml, kindly obtained from Professor M.E. Schwab, University of Zurich), Rolipram (5 μM, Sigma–Aldrich, Switzerland) and TTX (tetrodotoxin, 1 μM, Alomone, Israel) were added to the medium directly after the lesion of the cultures. The whole medium was exchanged twice per week with the respective compound diluted until the cultures were used for recordings. For the chondroitinase treatment (chABC, 0.2–2 U/ml, amsbio,

Table 1. Characterization of spontaneous bursting activity under standard conditions and disinhibition. In cultures without a lesion, the activity patterns under both conditions recorded at 22 and 36 DIV are in almost all parameters significantly different to the ones at 8 DIV. In general, burst rates are higher, bursts are shorter and the patterns are more regular after 3 weeks in culture. We found no significant changes between 22 and 36 DIV ($p > 0.05$). No significant differences were established between the bursting activity from cultures lesioned at 8 DIV and from cultures recorded at the same age (22 DIV) but without a lesion. Cultures lesioned at 21 DIV displayed under disinhibition less regular bursting than unlesioned cultures of the same age and than cultures lesioned at 8 DIV.

		No lesion						Lesion			
Age at recording		8 DIV	]	22 DIV	]	36 DIV	]	At 8 DIV 22 DIV	]	At 21 DIV 36 DIV	]
Burst rate (per min)	StdC	1.1 ± 0.1	]**	11.0 ± 1.0***	]***	11.2 ± 1.2***	]***	9.8 ± 1.3	]***	11.2 ± 1.9	]***
	Dis	0.5 ± 0.1		2.0 ± 0.1**		2.1 ± 0.1**		1.6 ± 0.2		2.0 ± 0.1	
Period (s)	StdC	71.9 ± 14.9	]**	6.0 ± 0.6***	]***	6.5 ± 1.0***	]***	7.5 ± 1.1	]***	7.4 ± 1.4	]***
	Dis	153.8 ± 19.5		31.7 ± 2.4***		28.9 ± 1.8***		42.3 ± 3.7		38.4 ± 3.4	
CV period (%)	StdC	43.1 ± 3.4	]***	69.8 ± 3.6***	]***	64.9 ± 3.6***	]**	69.0 ± 5.5	]***	76.7 ± 9.2	
	Dis	19.3 ± 3.7		40.1 ± 2.5***		48.4 ± 3.9***		44.7 ± 2.3		64.6 ± 2.4***,a	
Burst duration (s)	StdC	16.3 ± 2.5		1.34 ± 0.18***	]***	1.2 ± 0.3***	]***	1.4 ± 0.2	]***	1.1 ± 0.3	]***
	Dis	17.6 ± 3.7		6.2 ± 0.6*		6.8 ± 0.4**		8.3 ± 0.8		6.6 ± 0.7	
CV burst duration (%)	StdC	53.4 ± 7.6	]**	90.4 ± 13.3	]***	125.6 ± 19.7**	]**	84.2 ± 16.2	]***	98.6 ± 14.8	]***
	Dis	18.6 ± 2.8		28.3 ± 3.2		36.0 ± 5.0*		31.9 ± 2.8		35.7 ± 2.6	
Interval (s)	StdC	53.8 ± 16.2	]**	4.7 ± 0.6**	]***	5.4 ± 1.0**	]***	6.2 ± 1.1	]***	6.3 ± 1.1	]***
	Dis	136.3 ± 18.3		25.4 ± 2.3***		22.0 ± 1.8***		33.9 ± 3.4		31.7 ± 3.2	
CV interval (%)	StdC	59.5 ± 4.8	]***	82.0 ± 3.8**	]***	73.9 ± 4.6		79.7 ± 5.7	]**	87.2 ± 10.9	
	Dis	22.3 ± 4.0		50.4 ± 3.4***		62.2 ± 5.4***		56.4 ± 3.1		79.7 ± 2.8**,a	
Spike rate (events/s/el.)	StdC	0.4 ± 0.1		3.2 ± 0.7***		2.9 ± 0.4***		2.6 ± 0.3		2.9 ± 0.4	
	Dis	0.5 ± 0.1		2.3 ± 0.7*		3.3 ± 0.9*		3.1 ± 0.5		3.3 ± 0.4	
n	StdC	9		10		9		11		9	
	Dis	7		9		8		18		18	

Stars nearby values: no lesion 22 DIV vs no lesion 8 DIV and no lesion 36 DIV vs no lesion 8 DIV; Stars nearby bracket: significant differences between standard condition (StdC) and disinhibition (Dis).

CV, coefficient of variation; el, electrode.

[a] Lesion at 21 DIV vs no lesion 36 DIV and vs lesion at 8 DIV.

* $p < 0.05$.

** $p < 0.01$.

*** $p < 0.001$.

England), 10 µl chABC in phosphate-buffered saline (PBS) were dripped onto the lesion site. The cultures were then placed into the incubator on a rotation table for 1 h. Subsequently, 3 ml of medium were added to the cultures before putting them back into the roller drums. This procedure was repeated every day during the first week of culturing and every third day during the following culture period.

Antibodies

The following first antibodies were used: SMI-31, 1:1000, abcam; SMI-32, 1:1500, Covance; anti-β-III-tubulin, 1:2000, Promega; NeuN, 1:200, Millipore; GFAP, 1:500, abcam; MOG, 1:1000, Santa Cruz Biotechnology; PLP, 1:500, abcam; SMI-94, 1:1000, abcam; anti-Nogo-A, 1:100, R&D Systems; anti-NgR-1, 1:250, abcam.

SMI-32 is a marker of non-phosphorylated neurofilaments. It is widely used to identify motoneurons but has been shown to stain other cells as well (Tsang et al., 2000). On the other hand SMI-31 labels phosphorylated neurofilaments and therefore axons of a variety of different cell types but rarely motoneurons (Tsuji et al., 2005). Anti-β-III-tubulin is a marker for dividing and postmitotic neurons (Menezes and Luskin, 1994; Memberg and Hall, 1995). NeuN stains the neuronal nucleus of differentiated neurons (Cifra et al., 2012). Anti-GFAP recognizes glial fibrillary acidic protein, typically expressed by astrocytes. SMI-94 stains against myelin basic protein (MBP) which is expressed already early during development. Together with PLP and its splice variant DM-20, MBP belongs to the most abundantly occurring lipids in CNS myelin (Quarles et al., 2006). MOG emerges around birth *in vivo* in newborn rats and is exclusively expressed in the CNS. It stains the outer surface of the myelin sheath and the plasma membrane of differentiated oligodendrocytes (Coffey and McDermott, 1997).

Immunohistochemistry

Cultures were fixed in 4% paraformaldehyde in PBS (0.1 M, pH 7.4) for 1–2 h at 4 °C, rinsed three times with PBS at room temperature and stored in PBS at 4 °C until used. They were blocked in 3% serum (goat or horse, Gibco BRL, Switzerland), 0.5% bovine serum albumin (Sigma–Aldrich, Switzerland) and 0.3% Triton X-100 (Merck, Germany) in PBS for 1 h at room temperature. Subsequently, the first antibody was diluted in blocking solution and applied overnight at 4 °C. Cultures were rinsed three times with PBS before the second antibody (AlexaFluor488, 1:1000; AlexaFluor568, 1:500; both Invitrogen) was added for 1–2 h at room temperature. After rinsing three times with PBS, cultures were incubated in 6-diamino-2-phenylindole (DAPI, 1:2000, Chemicon) for 2 min, rinsed again in PBS and finally, mounted on object plates and coverslipped by Mowiol (Sigma–Aldrich, Switzerland).

To count the number of fibers crossing the lesion site, cultures were stained with SMI-31 or anti-β-III-tubulin antibody about 2–3 weeks after applying lesions (lesions in young cultures at 7–9 DIV and in old cultures at 21–23 DIV). Light microscope pictures of the same magnification were used to count the number of SMI-31-positive fibers (Carl Zeiss, Germany; color camera: Visitron Systems, USA). We draw a vertical line in the center of the lesion and counted all the axons crossing this line. For each culture the result is expressed as crossing axon per picture. For the anti-β-III-tubulin staining, fibers were counted using both confocal imaging (Leica TCS SP2) and light microscopy. Several cultures were examined with both methods getting almost identical values. When checking the culture thickness at the lesion site we found no evidence for a decrease with age (young: 193.2 ± 21.6 µm, $n = 6$; old: 178.8 ± 13.7, $n = 8$, $p = 0.56$). Moreover, most crossing fibers were in the same layer of a culture allowing us to get sharp pictures of stained fibers with the light microscope. Therefore, values from both measurement techniques were taken together for β-III-tubulin-positive fibers. For each culture, the result is expressed as crossing fibers per culture.

Statistics

Results are expressed as mean ± standard error of the mean. Values were set as significant where $p < 0.05$ (*), very significant where $p < 0.01$ (**), and extremely significant where $p < 0.001$ (***). Statistics were calculated from raw data with InStat (GraphPad Software Inc., USA). Groups passing the normality test were assessed with parametric tests and the other with non-parametric tests. In particular, differences among two groups were evaluated using unpaired *t*-tests and the unpaired, non-parametric, two-tailed Mann–Whitney test (except in Fig. 5D, E paired, non-parametric, two-tailed Wilcoxon matched-pairs signed ranks test) and among several groups with a one-way analysis of variance (ANOVA) or non-parametric, two-tailed Kruskal–Wallis tests.

RESULTS

For our experiments we cultured two transversal spinal cord slices derived from E14 rat embryos about 300 µm apart from each other on MEAs. The activity was recorded between 8 and 42 DIV and was usually organized in bursts as reported before for single slice cultures (Tscherter et al., 2001; Czarnecki et al., 2008). The use of MEAs allowed us to determine for both slices within a culture the starting time, starting point, duration and propagation of bursts. To evaluate the functional connectivity between the two slices we calculated the percentage of occurring synchronized bursts. Recordings were first taken under standard conditions and afterward under disinhibition by blocking synaptic inhibition with strychnine and gabazine. This led in general to more periodic activity with prolonged bursts and burst intervals, allowing for a more precise analysis of the data (see Table 1; Streit et al., 1991).

Electrophysiological and immunohistochemical characterization at 8 DIV

First of all, we recorded the spontaneous activity at 8 DIV. At this time, the slices have expanded in size and have grown together along the sides facing each other (Fig. 1B). Remarkably, we found that already at 8 DIV the bursting activity between the two slices is highly synchronized (Fig. 1C, D). We calculated 92.0 ± 4% synchronized bursts under standard conditions (n = 12) and 98.9 ± 0.7% under disinhibition (n = 16). This means that these cultures display an excellent ability to recover from the slice preparation. In both conditions, the propagation of bursts was bi-directional. Roughly 75% of the synchronized bursts originated in one side (standard condition: 72.6 ± 6.1%; disinhibition 77.8 ± 5.1%) and the remaining 25% bursts in the other (Fig. 1E, F). Additionally, we found a significantly lower mean burst rate with bursts having more events in the initial phase under disinhibition than under standard conditions (Table 1). Nonetheless, the activity patterns of the two conditions looked similar as bursts had similar durations and the activity under standard conditions was quite regular. We used the MEAs further to induce bursts by electrical stimulation. In all cultures tested, we found ventrally and dorsally only a few electrodes that were able to trigger bursts in a slice. These bursts reliably propagated to the other slice.

In addition to the electrophysiological analysis of the bursting activity we characterized the area, where the two spinal cord slices fused together, by means of immunofluorescent staining at a culture age of 8 DIV (Fig. 2). Overall, we found similar results compared to the study from Cifra et al. (2012) in which they investigated, among other things, the developmental profile of neurons and glia in organotypic spinal cord cultures at three different ages. We found that the area around the fusion site contained neurons, axons (both β-III-tubulin-positive), oligodendrocytes, myelin (SMI-94, PLP and MOG-positive) and astrocytes (GFAP-positive).

In an attempt to label motoneurons we used the SMI-32 antibody against non-phosphorylated neurofilament (Bonnici and Kapfhammer, 2008; Cifra et al., 2012). We found numerous SMI-32-positiv cell bodies and a huge network of fibers distributed within and between the slices, opening the possibility that motoneurons may also contribute to the functional connection between the slices (see 'Discussion').

Since SMI-32 was also shown to stain dorsal root ganglion (DRG) cells we used this antibody to check for the occurrence of such neurons in our cultures. We identified SMI-32 positive cells with the characteristic morphology of DRG neurons at the borders of the cultures (Fig. 2G, G1).

To rule out that DRG cells are crucial in the functional connection of the two slices, cultures were prepared

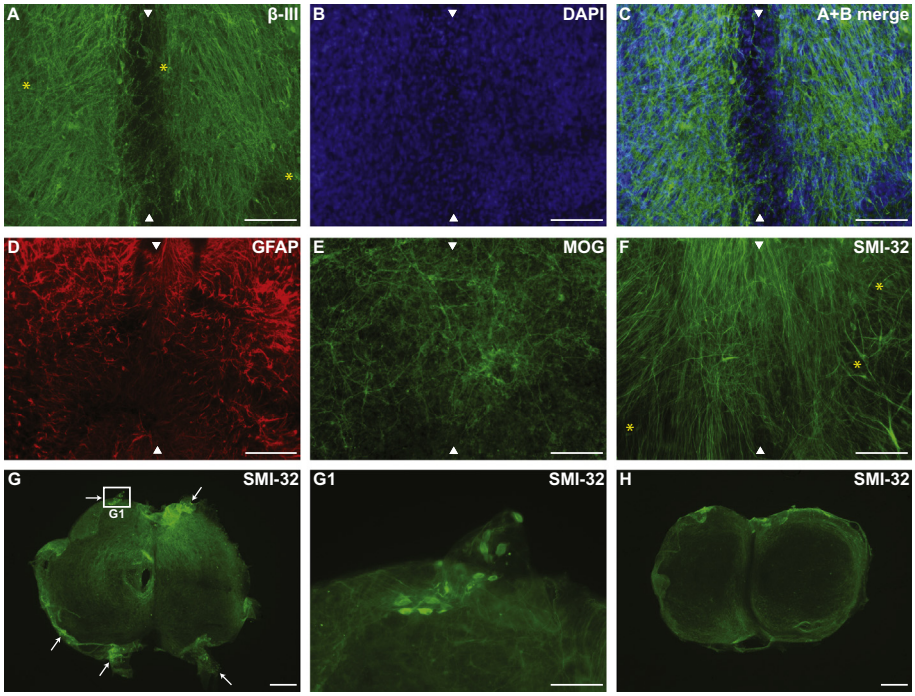

Fig. 2. Immunofluorescent characterization at 8 DIV. The area where the two spinal cord slices fused is indicated by two arrowheads in A–F. Examples of stained cell bodies are marked with stars. (A) Staining of neuronal fibers and mature neuronal cell bodies with anti-β-III-tubulin. Several fibers cross the fusion site. There are some mature neurons in the fusion site and within the slices.(B) DAPI staining of the same area visible in A. (C) Only a few of the DAPI + cell bodies in the fusion site display mature neuron identity. (D) Abundant expression of GFAP within the slices but only a few astrocytes are visible in the fusion site. (E) Identification of myelin and oligodendrocyte cell bodies by MOG staining. (F–H) Staining of non-phosphorylated neurofilament H with anti-SMI-32. (F) Many fibers cross the fusion site, cell bodies are located within the slices. (G) Identification of DRG neurons at the borders of the slices (arrows). The rectangle is magnified in (G1). (H) Example of a culture, from which the DRGs were removed during the preparation process. We did not find evidence for DRG cell bodies at the borders or within the slices. Scale bars A–C, E, F, G1 = 100 μm; D = 200 μm; G, H = 400 μm.

without any attached spinal ganglia. The absence of DRG cells in such cultures was confirmed by immunohistochemical staining (Fig. 2H). As pointed out below, the lack of DRG cells did not alter burst synchrony, demonstrating that these cells are not essential for the propagation of bursts from one side to the other.

Decrease of functional regeneration with age

It has been demonstrated that organotypic cultures of hippocampus and also spinal cord derived from postnatal mice pups show abundant axonal recovery of lesioned fibers. However, this ability for spontaneous regeneration is lost in an age-dependent manner (Prang et al., 2001; Bonnici and Kapfhammer, 2008). In this context, we re-separated the two originally autonomous slices in a time window of 8–28 DIV at their fusion site and therefore cut all the formed connections between them. The lesion had a maximal width of 300 µm. 14–21 days after setting the lesion we determined the mean percentage of synchronized bursts in groups of usually 10 cultures per lesion day. This percentage decreased with increasing age of the cultures on the lesion day (Fig. 3A, B). We recorded 50.4 ± 7% (n = 11) burst synchronization from young cultures that received the lesion at 8 DIV under standard conditions and 95.3 ± 2.1% (n = 17) under disinhibition but less than 12% from old cultures lesioned after 18 DIV under both conditions. In the young synchronized cultures, bursts propagated again in both directions whereby 81.2 ± 4.1% of the bursts originated in one side under standard condition and 70.4 ± 3.6% under disinhibition. In addition, electrical stimulation induced bursts in young as well as in old cultures. They propagated like spontaneous bursts to the other side but only in the young functionally connected cultures.

We can exclude that DRG cells are essential in the functional reconnection in the young cultures (lesioned at 8 DIV) as we found 100% synchronized burst under disinhibition in cultures prepared without any attached spinal ganglia (n = 7).

The decreased ability for functional recovery with age may be caused by deterioration in old cultures or by a reduced propensity to generate bursts. To exclude these possibilities, we compared the bursting activity of old cultures (lesioned at 21 DIV) with the young ones (lesioned at 8 DIV) and also with unlesioned cultures of the same age (Table 1). The number of bursts per minute was under standard conditions tremendously higher at 22 and 36 DIV than at 8 DIV. In addition, the burst lengths were shorter and the activity patterns much more irregular. Disinhibition of cultures at these ages increased the burst duration and decreased also the coefficient of the burst period. Nevertheless, the percentage of synchronized bursts did not change with age and was around 80% under standard conditions (22 DIV: 80.9 ± 5.8%, n = 11; 36 DIV, 81.7 ± 5.4%, n = 9) and around 100% under disinhibition (22 DIV, 100.0 ± 0.0%, n = 15; 36 DIV: 98.2 ± 1.0%, n = 13). To summarize, we found in unlesioned cultures no significant changes between 22 and 36 DIV (all

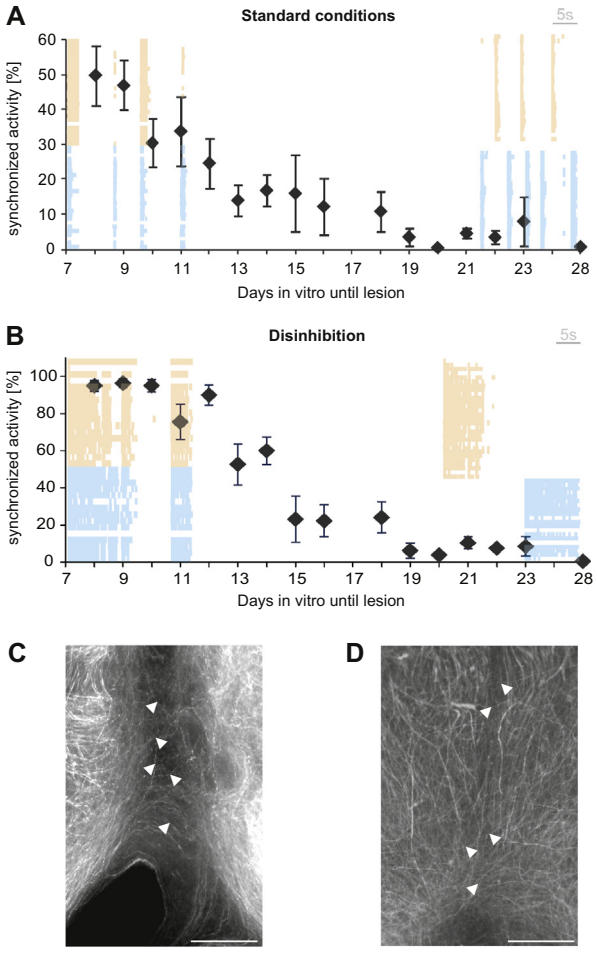

Fig. 3. Functional recovery decreases with age in spinal cord slice cultures. (A, B) Mean percentage of synchronized activity plotted for each individual day of lesion. Representative cutouts of raster plots for cultures lesioned at a young age (7–9 DIV) and old age (> 19 DIV) are displayed in light and dark gray in the background. (A) Standard conditions, (B) Disinhibition. (C, D) Axons were stained with SMI-31 antibody. Independent of the age at which the lesion was performed (in C) at 8 DIV, in (D) at 22 DIV) it is possible to identify fibers crossing the lesion site (arrowheads). Scale bar = 150 µm.

p > 0.05) under both recording conditions, neither in the bursting pattern nor in the synchronization of bursts.

These results reveal that for standard conditions, the percentage of burst synchronization of cultures lesioned at 8 DIV is significantly lower from the one of cultures without lesion recorded at the same age (22 DIV: 80.9 ± 5.8% vs with lesion at 8 DIV 50.4 ± 7%, p < 0.01). However, we did not find any difference in the burst synchronization under disinhibition (both around 100%) and in the bursting pattern between these two groups (Table 1). Cultures lesioned at 21 DIV displayed a drastic decline of the burst synchronization compared to the cultures of the same age without any lesion in both recording conditions (p < 0.001). Their bursting activity was also more irregular than in unlesioned cultures or than in cultures lesioned at 8 DIV (Table 1). Importantly, there were no significant differences in the burst rate, burst duration and number of events detected in both recording conditions between

cultures lesioned at 21 DIV and cultures of the same age or those lesioned at 8 DIV. These findings indicate that the propensity to generate bursts in old cultures is not diminished after setting a lesion and that the reduction of synchronized activity comes from an inability to reestablish functional connectivity between the two slices with increasing culture age.

Discrepancy between functional and morphological results

A decrease of fibers crossing through the lesion may explain the observed reduction in functional regeneration. To investigate this possibility, we stained the cultures after the recordings with SMI-31 antibody which labels phosphorylated neurofilament H that is substantially expressed in axons and with anti-β-III-tubulin antibody that labels neuronal cell bodies and neurites. Unexpectedly, when visually counting the number of axons crossing from one slice to the other, we found no evidence for a decrease in the average number of crossing axons in young (lesion at 7–9 DIV) vs old (lesion at 21–23 DIV) cultures (SMI-31: Fig. 3C, D, young: 7.5 ± 3, $n = 4$, old: 8.75 ± 2.1, $n = 8$, $p = 0.67$; anti-β-III-tubulin: young: 9 ± 1.7, $n = 5$, old: 11.5 ± 1.9, $n = 6$, $p = 0.36$, see methods).

In summary, burst synchronization between the two slices decreases to values below 12% between lesion days 11 and 19, although there is no evidence for a decrease in the number of axons crossing the lesion. We conclude that we can functionally investigate the regeneration of spinal cord cultures by using the amount of synchronized bursts between the two slices.

Activity effects on the intrinsic regeneration of young cultures

To investigate the speed with which young cultures can regenerate, we set the lesions at 6 DIV and recorded the activity of the slices 1–3 days later. While we found an incomplete activity synchronization on the first day (52.9 ± 13.5% under disinhibition, $n = 10$), 91.7 ± 8.3% burst synchronization was already reached on the second day ($n = 6$).

To determine whether this fast recovery of axonal connections is activity dependent we added TTX to the culture medium immediately after setting the lesion at 8 DIV and recorded the activity 4–6 days later. TTX exposure significantly reduced synchronization under disinhibition while the observed decrease under standard condition was not significant (Fig. 4A, B). Interestingly, in cultures without lesion, TTX treatment at 8 DIV for 4–6 days significantly reduced synchronization under both recording conditions (Fig. 4C, D).

Mixed cultures – activity bursts can propagate in both directions

So far, our findings suggest that the regeneration potential is high in young cultures lesioned up to an age of 10 DIV and is almost completely lost in old cultures

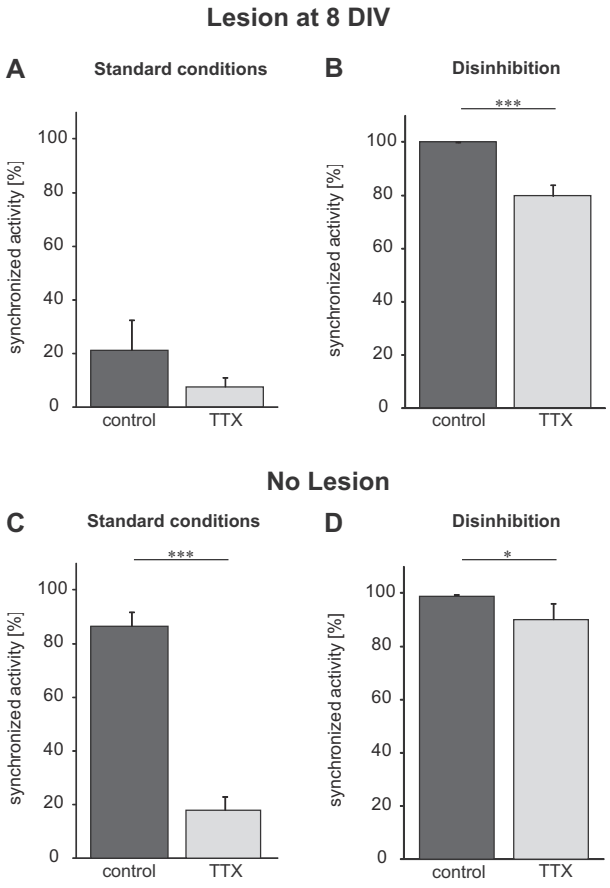

Fig. 4. The fast regeneration process of young slices is partially activity dependent. (A, B) TTX application directly after the lesion reduced the percentage of synchronized activity recorded 4–6 days later compared to the control group. The effect is significant under disinhibition. Standard conditions: control $n = 8$, TTX $n = 5$; Disinhibition: control $n = 10$, TTX $n = 10$. (C, D) TTX application from 8 DIV up to the recording but without performing a lesion results in a significant difference under standard conditions (C) as well as under disinhibition (D). Standard conditions: control $n = 7$, TTX $n = 6$; Disinhibition: control $n = 16$, TTX $n = 6$.

lesioned after 18 DIV. To investigate this further we studied the burst synchronization in mixed cultures consisting of an old and a young slice. We prepared two culture series at a time interval of 2 weeks, one of them from ubiquitously GFP-expressing embryos. This setup allowed us to move a 7-day-old slice next to a 21-day-old slice after setting the lesion (Fig. 5A). We recorded an average of 29.8 ± 5.3% of synchronized bursts under standard conditions ($n = 27$) and 62.6 ± 5.7% under disinhibition ($n = 35$, Fig. 5B, C). We conclude that under standard conditions there is no difference in regenerative ability between mixed and young cultures (lesion at 7–9 DIV: 37.2 ± 4.5%, $n = 26$, $p > 0.05$) but mixed cultures regenerate significantly better than uniform old cultures (lesion at 21–23 DIV: 4.0 ± 1.2%, $n = 67$, $p < 0.001$). Under disinhibition, mixed cultures regenerate significantly better than uniform old cultures (9.5 ± 2.4%, $n = 65$, $p < 0.001$) and significantly less well than uniform young cultures (96.3 ± 1.5%, $n = 30$, $p < 0.05$).

To check for a possible dominance of the young or the old slice we looked again at the direction of activity propagation. Cultures with a low percentage of synchronized bursts (< 10%) were excluded from this analysis. Under standard conditions we found a mean of 54.4 ± 7.6% of burst which had their origin in the young slice and propagated into the old slice. Significantly less of the bursts starting in the old slice propagated into the young slice (26.2 ± 8.3%, $n = 18$, $p < 0.05$ Fig. 5D). Under disinhibition 82.3 ± 5.0% of the bursts originating in the young slice spread into the old slice, while 51.8 ± 8.0% of the bursts ran in the opposite direction ($n = 29$, $p < 0.01$, Fig. 5E). Together these findings suggest that young slices have a high potential to form functional circuits with old slices after lesions, although recovery is stronger between two young slices. On the other hand, axons of old slices have lower potential to grow into young slices but almost no functional regeneration takes place between two old slices.

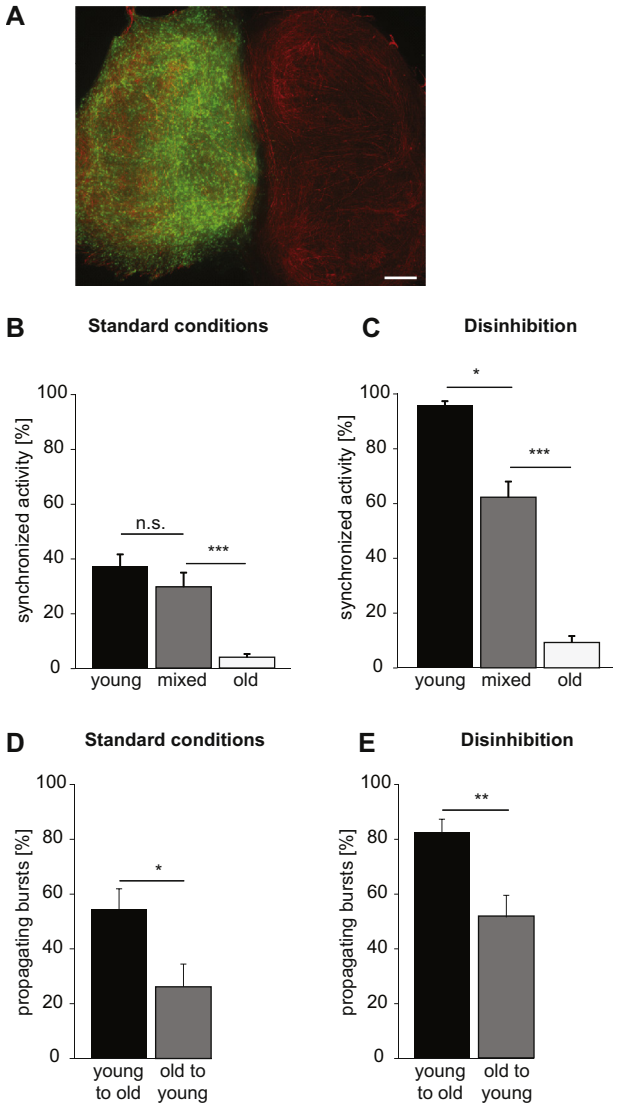

Fig. 5. Replacing an old slice with a young slice after the lesion improves functional recovery. A) Fluorescent picture of a mixed culture. The young slice is GFP positive. Axons of the whole culture are stained with SMI-31 antibody. Scale bar = 400 μm. (B, C) Mixed cultures regenerated better compared to uniform old cultures but worse than uniform young cultures, (B) Standard conditions, (C) Disinhibition. (D, E) Mean percentage of bursts initiated in one slice and followed by a burst in the other one. Cultures with percentages of synchronized bursts lower than 10% were excluded from this analysis (see 'Experimental procedures' for details). Under both recording conditions, a higher percentage of bursts propagated from the young to the old slices than vice versa.

Rolipram promotes functional recovery *in vitro*

Our findings revealed a low intrinsic regeneration potential for old cultures lesioned at 19 DIV or later, suggesting that they can be used as a model to investigate strategies to improve functional regeneration. So far, functional recovery was only studied *in vivo*, mostly in the corticospinal tract. The phosphodiesterase inhibitor Rolipram has been shown to promote regeneration in different fiber tracts (Nikulina et al., 2004; Bonnici and Kapfhammer, 2008) *in vitro* and *in vivo*. To assess our model, we therefore treated the cultures with Rolipram directly after setting the lesion at 21 DIV. Under disinhibition Rolipram significantly increased burst synchronization compared to the control group (Fig. 6B: Rolipram: 38.2 ± 4.6%, $n = 45$; controls: 10.5 ± 3.2%, $n = 47$, $p < 0.001$). We did not observe a significant increase under standard conditions (Fig. 6A: Rolipram: 6.7 ± 1.7%, $n = 45$; controls: 4.6 ± 1.5%, $n = 49$, $p > 0.05$). This finding may be explained by an augmentation of the number of fibers passing from one side to the other. However, we did not find a significant change in the number of anti-β-III-tubulin-positive fibers crossing through the lesion (control: 11.5 ± 1.9, $n = 6$; with Rolipram: 10 ± 1.4, $n = 5$, $p = 0.56$).

Blocking glial growth inhibitors does not improve functional recovery

The applications of substances that interfere with glial growth inhibitors (e.g. Nogo-A antibodies, NEP1–40, chABC) have been found to improve regeneration after SCI (Bregman et al., 1995; Benowitz et al., 1999; Bradbury et al., 2002; GrandPré et al., 2002; Nikulina et al., 2004). None of these specified agents significantly increased burst synchronization in our cultures, either under standard conditions (Fig. 6A: anti-Nogo-A: 8.0 ± 3.9%, $n = 8$; NEP1–40: 3.7 ± 2.6%, $n = 9$; chABC: 1.3 ± 0.7%, $n = 9$) or under disinhibition (Fig. 6B: anti-Nogo-A: 12.2 ± 5.1%, $n = 6$; NEP1–40: 14.2 ± 6.6%, $n = 9$; chABC: 7.6 ± 2.7%, $n = 14$). Also Inosine, a player in the signal transduction pathway through which trophic factors stimulate axonal growth, did not improve burst synchronization (standard conditions: 13.4 ± 2.5%, $n = 66$; disinhibition: 1.8 ± 0.7%, $n = 63$).

Double labeling of 23-DIV-old cultures with anti-Nogo-A and NeuN antibody revealed that the Nogo-A protein is abundantly expressed in the cultures but not localized on mature neurons (Fig. 6C–E). In contrast, we did not detect Nogo receptor 1 (NgR-1, Fig. 6F, G) in the embryonic cultures whereas we found expression in the ventral

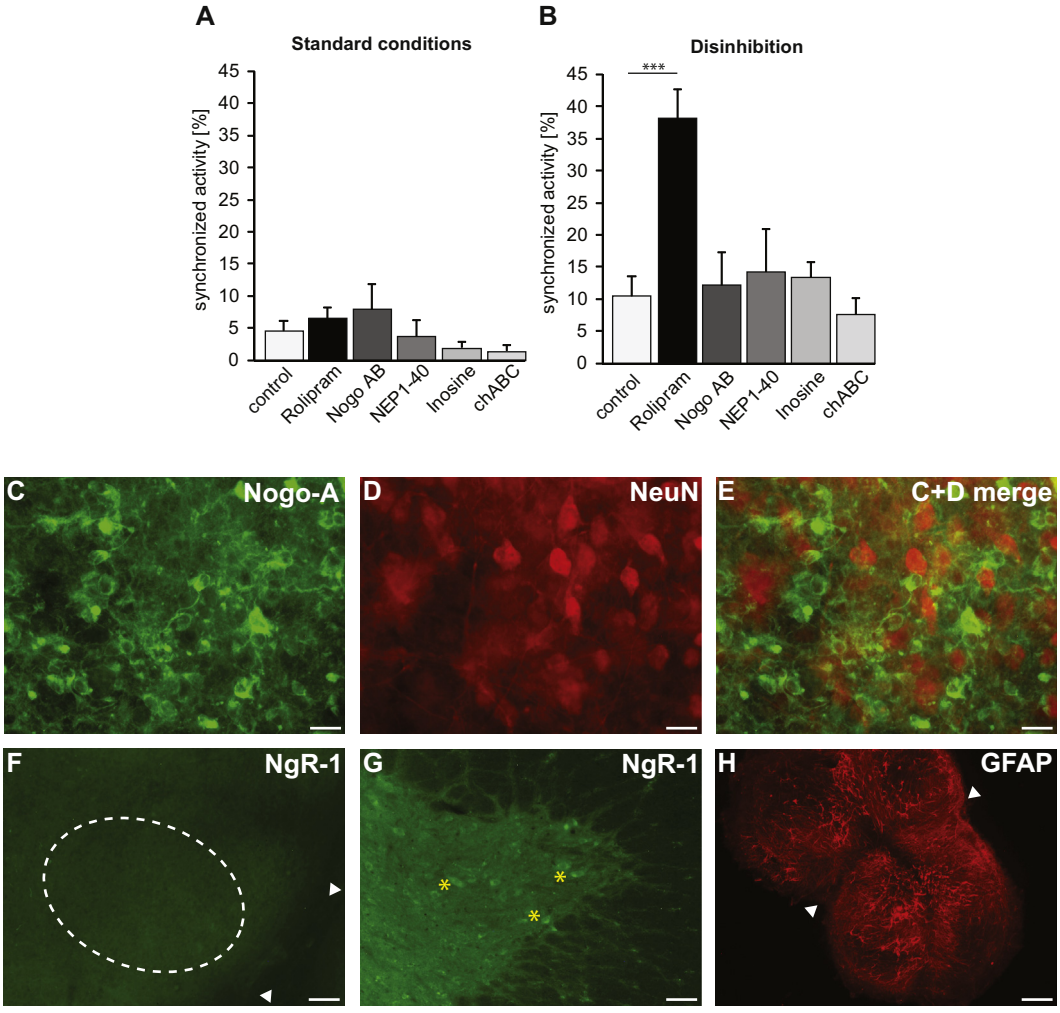

Fig. 6. Pharmacological treatment of spinal cord slice cultures lesioned at 21 DIV. (A) Under standard conditions neither of the applied agents revealed a positive effect on functional regeneration compared to the control group. AB = Antibody (B) Under disinhibition, Rolipram [5 μM] significantly improved functional regeneration over the control group (ctrl: 10.5% ± 3.2%, Rolipram: 38.2% ± 4.6%). (C–E) Double labeling of 23-DIV-old cultures with anti-Nogo-A and anti-NeuN indicates that Nogo-A is abundantly expressed in our cultures but not on mature neurons. Scale bar = 20 μm. (F) We found no evidence for NgR-1 expression in 23-DIV-old embryonic cultures. Arrowheads indicate the fusion site between the two spinal cord slices. The dashed circle marks the ventral area of one slice. Scale bar = 80 μm. (G) Anti-NgR-1 labeling of a spinal cord slice from adult rat reveals positive cells in the ventral horn (examples marked with stars). Scale bar = 80 μm. (H) Staining of a 5-week-old culture, lesioned after 21 DIV with GFAP antibody revealed no indication of glial scar formation. Arrowheads mark the lesion site. Scale bar = 200 μm.

horn of spinal cord slices from adult rats, kindly obtained from Professor H.R. Widmer (University of Bern). Finally, we stained 36-DIV-old cultures, which were lesioned at 21 DIV against GFAP (Fig. 6H). We found no evidence for the formation of a glial scar between the two slices.

DISCUSSION

With this study we present evidence that organotypic spinal cord cultures of E14 rat embryos lose over time the ability to reestablish activity synchronization between two slices after lesion. This loss seems to be unrelated to a general failure of old axons to regenerate, emphasizing the need for the functional investigation of this connectivity. Raising intracellular cAMP levels with Rolipram or placing a young slice next to an old one both substantially increase functional regeneration. In mixed cultures activity bursts can propagate from the young into the old slice and vice versa. Moreover, we found that in young cultures the process of functional connection between spinal cord slices seems to be, at least partly, activity dependent.

Burst synchronization as a measure of functional regeneration

For our analysis we took advantage of the spontaneously occurring network activity bursts in the spinal cord slices. By using this method we can reliably quantify the extent of functional regeneration. Since we recorded from many points at the same time we were able to detect very accurately the origin of each burst which is crucial to define the direction of activity propagation. Our focus was on bursts with a certain minimal amount of activity. Therefore, it is possible that we missed regenerated

functional connections which were too weak to induce an activity level reaching this threshold.

The averaged burst synchronization recorded under standard conditions from cultures lesioned at 8 DIV reached two-thirds of the value recorded from cultures without lesion. We attribute this difference to less excitatory connections between the two slices in lesioned cultures. The percentage of burst synchronization recorded under disinhibition was generally higher than during standard conditions. Several factors can account for this result, for example an increase in the initial spike rate of bursts probably boosting the synaptic input to the adjacent side, the neutralization of potential inhibitory connections and general facilitation of burst generation (more hubs; Czarnecki et al., 2012) or the limitation of burst generation by the network refractory period following the previous burst (Darbon et al., 2002; Yvon et al., 2005). This limitation is less likely during disinhibition due to the low and regular burst rates. Altogether our findings suggest that the use of burst synchronization, especially during disinhibition, is a highly sensitive method to detect functionally relevant excitatory connections between two networks.

Functional recovery failure in the presence of apparently equal regeneration

Burst synchronization requires on one hand the capability to generate bursts in both slices and on the other hand, excitatory axonal connections between the two slices. The capability of burst generation was confirmed for all slices by the occurrence of spontaneous bursts. In addition, we did not observe a decrease of the burst rate and consequently of the propensity to generate bursts with increasing age. It is therefore surprising that the number of axons crossing the lesion site was roughly the same in the young cultures displaying a high amount of burst synchronization as in the old cultures displaying no or little burst synchronization. We do not know which of the crossing axons are functionally relevant. A previous study with networks of dissociated cells suggests that few axons are sufficient to support the propagation of bursts (Yvon et al., 2005). Therefore, it can be possible that we missed the changes in the number of functionally relevant axons with the applied methods. Alternatively the lack of burst synchronization in old cultures may be more related to a lack in synapse formation than to insufficient axonal growth.

We can exclude that DRG neurons play a role in functional regeneration in our model because cultures prepared from slices from which the spinal ganglia have been removed show equal percentages of synchronized activity compared to cultures with DRGs left attached. In contrast, axons of motoneurons might contribute to the functional connection between the two slices. As motoneurons have not reached their typical large size at 8 DIV (Avossa et al., 2003), we cannot verify that all SMI-32 positive cell bodies are indeed motoneurons. It has been reported that the SMI-32 staining is not exclusive to motoneurons and that a prominent amount of neuronal processes stain positive for the non-phosphorylated neurofilament throughout the spinal cord (Tsang et al., 2000). Therefore, we are not able to decipher if and how many motoneuron axons contribute to the connection between the two spinal cord slices and whether they are functionally relevant.

Functional recovery occurs during a similar time window as in the *in vivo* situation

In vivo studies in different animal models have shown that embryonic and early postnatal animals are able to heal from spinal injury but that this ability is lost during a critical phase of the developmental transition (Blackmore and Letourneau, 2006). In rats this transition was reported to occur before 15 days of age (Weber and Stelzner, 1977). In our culture system the ability for functional regeneration decreases between 11 and 19 DIV. This time frame would correspond to P2 to P11 *in vivo*. Therefore, we propose that the decrease in recovery in our culture model occurs during a similar time window as in the *in vivo* situation. This statement is supported by morphological and physiological studies analyzing parameters such as cell shape and changes in protein expression in organotypic spinal cord cultures. They were developmentally equivalent to the corresponding *in vivo* age (Avossa et al., 2003; Bonnici and Kapfhammer, 2008; Cifra et al., 2012). Similar conclusions were drawn for organotypic cultures from other central nervous system areas, for example, the hippocampus (de Simoni et al., 2003; Orlando et al., 2012).

No involvement of the classical myelin and glial inhibitors of axonal growth

A major reason for the failure of axons to regenerate after SCI has been attributed to inhibitory cues in central nervous system myelin, particularly to the protein Nogo-A. Treatment with a Nogo-A antibody or blockage of NgR-1 with the artificial peptide NEP1-40 after SCI has been shown to improve functional regeneration *in vivo* many times (Bregman et al., 1995; Merkler et al., 2001; GrandPré et al., 2002; Li and Strittmatter, 2003). However, we found no effect of the Nogo-A antibody or NEP1-40 peptide on burst synchronization. We were able to confirm the presence of the Nogo-A protein in our culture by immunohistochemical staining whereas we found no expression of NgR-1. These findings suggest that the neurons in our cultures are insensitive to Nogo-A inhibition due to a lack of NgR-1 receptors. This hypothesis is in line with the finding of Bareyre et al. (2004) who did not observe a significant enhancement of the formation of detour circuits in the spinal cord after treatment with Nogo-A antibody.

Other well known inhibitors of axonal growth are CSPGs which are secreted by reactive astrocytes forming the glial scar after spinal cord trauma *in vivo*. A strategy to antagonize such inhibition is the degradation of CSPGs by chABC (Bradbury et al., 2002). Again, we did not observe a significant improvement of functional regeneration compared to the control group. This finding may be due to an insufficient amount of CSPG

degradation since our protocol of chABC application did not allow a persistently high concentration of the substance during the period of regeneration. On the other hand, immunohistochemical staining revealed no evidence for a glial scar with increased number of reactive astrocytes around the lesion area (Fig. 6H).

Altogether, our results present no evidence for a major involvement of the classical myelin and glial inhibitors of axonal growth in the loss of functional regeneration in our cultures. Our finding that the number of crossing axons was equal in old and young cultures fits to the hypothesis that axonal growth inhibition is not involved in the loss of functional regeneration.

State of neuronal maturation

In addition to an inhibitory environment, the state of neuronal maturation seems to influence the process of axonal regeneration. In this context, strong focus was set on the cAMP level, which is increased after injury and is lower in old neurons lacking the ability to functionally regenerate compared to young neurons which are still capable of recovery (Cai et al., 2001; Qiu et al., 2002). It was discovered that increasing the cAMP level in neurons after SCI by the application of Rolipram increases the regenerative ability *in vivo* (Nikulina et al., 2004). We were able to reproduce this finding in our culture model.

Our finding that old cultures can form functional connections to young cultures to some extent shows that the loss of functional recovery in old cultures cannot be entirely explained by a developmental loss of axonal outgrowth. Indeed it is known that adult central nervous system axons can regenerate but are limited in their ability to do so. One of the most prominent studies to underline this statement was performed by David and Aguayo (1981) in which they transplanted peripheral into central nervous tissue and demonstrated axonal outgrowth between brainstem and spinal cord through sciatic nerve ''bridges''.

In another attempt to promote functional regeneration in old cultures, we treated them with Inosine, which affects the signal transduction pathway through which trophic factors stimulate axon growth (Irwin et al., 2006). However, the effect of Inosine on functional regeneration is controversial. In agreement with another report (Steward et al., 2012), we did not find a significant improvement in functional recovery.

Synaptic plasticity – a possible hypothesis

Since the effects of glial inhibitory cues and the state of neuronal maturation, both of which influence axonal growth, cannot fully explain the loss of functional recovery in the lesioned old cultures we hypothesize that the process of synapse formation and synaptic plasticity is involved as well. Synaptic plasticity has been shown to take place after SCI (Tan and Waxman, 2012). Furthermore, spontaneous activity in the spinal cord influences the expression pattern of axon guidance cues and thereby has an effect on axonal pathfinding of motor neurons (Hanson and Landmesser, 2004). Blocking spontaneous activity bursts in our cultures by adding TTX to the culture medium significantly reduced functional regeneration under disinhibition. We also observed a major reduction of synchronized activity after TTX treatment even in absence of any lesion. Therefore, it is possible that axonal pathfinding and synapse formation of intraspinal neurons can be similarly affected by spontaneous activity bursts. This idea is further supported by the fact that the spontaneous bursting activity is different between 8 DIV and 21 DIV. Therefore diverse plasticity mechanisms may take place after lesion and affect functional recovery. This hypothesis would also explain our finding that the loss of functional recovery is not accompanied by a corresponding loss of axonal connections between the slices. To what extent synaptic plasticity is involved in functional recovery of burst synchronization remains to be investigated.

Acknowledgments—We thank Ruth Rubli for the preparation and maintenance of the slice cultures, Professor Hans Peter Clamann for the revision of the manuscript, Professor Stephen Leib for providing the GFP+ rats, Professor Martin Ernst Schwab for providing the Nogo-A antibody, Professor Stephan Rohr for the allocation of his microscope, Professor Walter Martin Senn for the fruitful discussions on the algorithm to calculate the randomly occurring bursts, Professor Thomas Nevian for the confocal imaging and Professor Hans Rudolf Widmer for the help with the immunohistochemical stainings.

This work was supported by the Swiss National Foundation (n° 3100A0-120327 and 31003A_140754/1).

REFERENCES

Avossa D, Rosato-Siri MD, Mazzarol F, Ballerini L (2003) Spinal circuits formation: a study of developmentally regulated markers in organotypic cultures of embryonic mouse spinal cord. Neuroscience 122:391–405.

Bareyre FM, Kerschensteiner M, Raineteau O, Mettenleiter TC, Weinmann O, Schwab ME (2004) The injured spinal cord spontaneously forms a new intraspinal circuit in adult rats. Nat Neurosci 7:269–277.

Benowitz LI, Goldberg DE, Madsen JR, Soni D, Irwin N (1999) Inosine stimulates extensive axon collateral growth in the rat corticospinal tract after injury. Proc Natl Acad Sci U S A 96:13486–13490.

Blackmore M, Letourneau PC (2006) Changes within maturing neurons limit axonal regeneration in the developing spinal cord. J Neurobiol 66:348–360.

Blesch A, Yang H, Weidner N, Hoang A, Otero D (2004) Axonal responses to cellularly delivered NT-4/5 after spinal cord injury. Mol Cell Neurosci 27:190–201.

Bonnici B, Kapfhammer JP (2008) Spontaneous regeneration of intrinsic spinal cord axons in a novel spinal cord slice culture model. Eur J Neurosci 27:2483–2492.

Bradbury EJ, Moon LDF, Popat RJ, von King R, Bennett GS, Patel PN, Fawcett JW, McMahon SB (2002) Chondroitinase ABC promotes functional recovery after spinal cord injury. Nature 416:636–640.

Bregman BS, Kunkel-Bagden E, Schnell L, Dai HN, Gao D, Schwab ME (1995) Recovery from spinal cord injury mediated by antibodies to neurite growth inhibitors. Nature 378:498–501.

Cai D, Qiu J, Cao Z, McAtee M, Bregman BS, Filbin MT (2001) Neuronal cyclic AMP controls the developmental loss in ability of axons to regenerate. J Neurosci 21:4731–4739.

Chen MS, Huber AB, van der Haar ME, Frank M, Schnell L, Spillmann AA, Christ F, Schwab ME (2000) Nogo-A is a myelin-associated neurite outgrowth inhibitor and an antigen for monoclonal antibody IN-1. Nature 403:434–439.

Cifra A, Mazzone GL, Nani F, Nistri A, Mladinic M (2012) Postnatal developmental profile of neurons and glia in motor nuclei of the brainstem and spinal cord, and its comparison with organotypic slice cultures. Dev Neurobiol 72:1140–1160.

Coffey JC, McDermott KW (1997) The regional distribution of myelin oligodendrocyte glycoprotein (MOG) in the developing rat CNS: an in vivo immunohistochemical study. J Neurocytol 26: 149–161.

Courtine G, Song B, Roy RR, Zhong H, Herrmann JE, Ao Y, Qi J, Edgerton VR, Sofroniew MV (2008) Recovery of supraspinal control of stepping via indirect propriospinal relay connections after spinal cord injury. Nat Med 14:69–74.

Czarnecki A, Magloire V, Streit J (2008) Local oscillations of spiking activity in organotypic spinal cord slice cultures. Eur J Neurosci 27:2076–2088.

Czarnecki A, Tscherter A, Streit J (2012) Network activity and spike discharge oscillations in cortical slice cultures from neonatal rat. Eur J Neurosci 35:375–388.

Darbon P, Scicluna L, Tscherter A, Streit J (2002) Mechanisms controlling bursting activity induced by disinhibition in spinal cord networks. Eur J Neurosci 15:671–683.

David S, Aguayo AJ (1981) Axonal elongation into peripheral nervous system "bridges" after central nervous system injury in adult rats. Science 214:931–933.

de Simoni A, Griesinger CB, Edwards FA (2003) Development of rat CA1 neurones in acute versus organotypic slices: role of experience in synaptic morphology and activity. J Physiol (Lond) 550:135–147.

GrandPré T, Nakamura F, Vartanian T, Strittmatter SM (2000) Identification of the Nogo inhibitor of axon regeneration as a Reticulon protein. Nature 403:439–444.

GrandPré T, Li S, Strittmatter SM (2002) Nogo-66 receptor antagonist peptide promotes axonal regeneration. Nature 417:547–551.

Hanson MG, Landmesser LT (2004) Normal patterns of spontaneous activity are required for correct motor axon guidance and the expression of specific guidance molecules. Neuron 43:687–701.

Houle JD (1991) Demonstration of the potential for chronically injured neurons to regenerate axons into intraspinal peripheral nerve grafts. Exp Neurol 113:1–9.

Inoue H, Ohsawa I, Murakami T, Kimura A, Hakamata Y, Sato Y, Kaneko T, Takahashi M, Okada T, Ozawa K, Francis J, Leone P, Kobayashi E (2005) Development of new inbred transgenic strains of rats with LacZ or GFP. Biochem Biophys Res Commun 329:288–295.

Irwin N, Li Y, O'Toole JE, Benowitz LI (2006) Mst3b, a purine-sensitive Ste20-like protein kinase, regulates axon outgrowth. Proc Natl Acad Sci U S A 103:18320–18325.

Kottis V, Thibault P, Mikol D, Xiao Z, Zhang R, Dergham P, Braun PE (2002) Oligodendrocyte-myelin glycoprotein (OMgp) is an inhibitor of neurite outgrowth. J Neurochem 82:1566–1569.

Levine JM (1994) Increased expression of the NG2 chondroitin-sulfate proteoglycan after brain injury. J Neurosci 14: 4716–4730.

Li S, Strittmatter SM (2003) Delayed systemic Nogo-66 receptor antagonist promotes recovery from spinal cord injury. J Neurosci 23:4219–4227.

McKerracher L, David S, Jackson DL, Kottis V, Dunn RJ, Braun PE (1994) Identification of myelin-associated glycoprotein as a major myelin-derived inhibitor of neurite growth. Neuron 13:805–811.

Memberg SP, Hall AK (1995) Dividing neuron precursors express neuron-specific tubulin. J Neurobiol 27:26–43.

Menezes JR, Luskin MB (1994) Expression of neuron-specific tubulin defines a novel population in the proliferative layers of the developing telencephalon. J Neurosci 14:5399–5416.

Merkler D, Metz GA, Raineteau O, Dietz V, Schwab ME, Fouad K (2001) Locomotor recovery in spinal cord-injured rats treated with an antibody neutralizing the myelin-associated neurite growth inhibitor Nogo-A. J Neurosci 21:3665–3673.

Mukhopadhyay G, Doherty P, Walsh FS, Crocker PR, Filbin MT (1994) A novel role for myelin-associated glycoprotein as an inhibitor of axonal regeneration. Neuron 13:757–767.

Nikulina E, Tidwell JL, Dai HN, Bregman BS, Filbin MT (2004) The phosphodiesterase inhibitor rolipram delivered after a spinal cord lesion promotes axonal regeneration and functional recovery. Proc Natl Acad Sci U S A 101:8786–8790.

Orlando C, Ster J, Gerber U, Fawcett JW, Raineteau O (2012) Perisynaptic chondroitin sulfate proteoglycans restrict structural plasticity in an integrin-dependent manner. J Neurosci 32:18009–18017.

Prang P, Del Turco D, Kapfhammer JP (2001) Regeneration of entorhinal fibers in mouse slice cultures is age dependent and can be stimulated by NT-4, GDNF, and modulators of G-proteins and protein kinase C. Exp Neurol 169:135–147.

Prinjha R, Moore SE, Vinson M, Blake S, Morrow R, Christie G, Michalovich D, Simmons DL, Walsh FS (2000) Inhibitor of neurite outgrowth in humans. Nature 403:383–384.

Qiu J, Cai D, Dai H, McAtee M, Hoffman PN, Bregman BS, Filbin MT (2002) Spinal axon regeneration induced by elevation of cyclic AMP. Neuron 34:895–903.

Quarles RH, Macklin WB, Morell P (2006) Myelin formation, structure and biochemistry. In: Siegel GJ, Agranoff BW, Albers RW, Fisher SK, Uhler MD, editors. Basic neurochemistry: molecular, cellular and medical aspects. Philadelphia: Lippincott-Raven. p. 58–63.

Steward O, Sharp K, Yee KM (2012) A re-assessment of the effects of intracortical delivery of inosine on transmidline growth of corticospinal tract axons after unilateral lesions of the medullary pyramid. Exp Neurol 233:662–673.

Streit J, Spenger C, Lüscher H (1991) An organotypic spinal cord – dorsal root ganglion – skeletal muscle coculture of embryonic rat. II. Functional evidence for the formation of spinal reflex arcs in vitro. Eur J Neurosci 3:1054–1068.

Tan AM, Waxman SG (2012) Spinal cord injury, dendritic spine remodeling, and spinal memory mechanisms. Exp Neurol 235: 142–151.

Tsang YM, Chiong F, Kuznetsov D, Kasarskis E, Geula C (2000) Motor neurons are rich in non-phosphorylated neurofilaments: cross-species comparison and alterations in ALS. Brain Res 861:45–58.

Tscherter A, Heuschkel MO, Renaud P, Streit J (2001) Spatiotemporal characterization of rhythmic activity in rat spinal cord slice cultures. Eur J Neurosci 14:179–190.

Tsuji S, Kikuchi S, Shinpo K, Tashiro J, Kishimoto R, Yabe I, Yamagishi S, Takeuchi M, Sasaki H (2005) Proteasome inhibition induces selective motor neuron death in organotypic slice cultures. J Neurosci Res 82:443–451.

Wang KC, Koprivica V, Kim JA, Sivasankaran R, Guo Y, Neve RL, He Z (2002) Oligodendrocyte-myelin glycoprotein is a Nogo receptor ligand that inhibits neurite outgrowth. Nature 417:941–944.

Weber ED, Stelzner DJ (1977) Behavioral effects of spinal cord transection in the developing rat. Brain Res 125:241–255.

Xu XM, Guénard V, Kleitman N, Bunge MB (1995) Axonal regeneration into Schwann cell-seeded guidance channels grafted into transected adult rat spinal cord. J Comp Neurol 351:145–160.

Yvon C, Rubli R, Streit J (2005) Patterns of spontaneous activity in unstructured and minimally structured spinal networks in culture. Exp Brain Res 165:139–151.

(Accepted 23 December 2013)
(Available online 3 January 2014)